

# Influence of layer deformation on thermal quenching of exciton photoluminescence in short-period GaAs/AlAs superlattices

D V Korbutyak<sup>1</sup>, V P Klad'ko<sup>1</sup>, S G Krylyuk<sup>1</sup>, V G Litovchenko<sup>1</sup>,  
A V Shalimov<sup>2</sup> and A V Kuchuk<sup>2</sup>

<sup>1</sup> V Lashkarev Institute of Semiconductor Physics, National Academy of Sciences of Ukraine, Prospect Nauki 45, 03028, Kiev, Ukraine

<sup>2</sup> Institute of Electron Technology, Al Lotników 32/46, 02-668 Warsaw, Poland

E-mail: div47@isp.kiev.ua

Received 13 October 2003

Published 13 January 2004

Online at [stacks.iop.org/SST/19/475](http://stacks.iop.org/SST/19/475) (DOI: 10.1088/0268-1242/19/3/033)

## Abstract

High-resolution x-ray diffraction and photoluminescence experiments were carried out on short-period direct-gap GaAs/AlAs superlattices. Despite a small difference in the well and barrier thicknesses of the samples studied, both the deformation of superlattice (SL) layers caused by the lattice mismatch and thermal activation energy of non-radiative recombination were found to differ for the different samples. The correlation observed between the deformation reduction and the activation energy increase as the SL period decreases is discussed in the context of a configuration coordinate diagram.

## 1. Introduction

The small mismatch between the lattice constants of GaAs and AlAs ( $\sim 0.12\%$ ) is favourable for the growth of high-quality superlattices (SLs), free of misfit dislocations. For the GaAs/AlAs SLs, the influence of layer deformations caused by the lattice mismatch for the two materials on the energy bands is much weaker as compared to the confinement effect. Nevertheless, such an influence still exists. It is especially important for the type-II GaAs/AlAs SLs in which a low compressive in-plane strain of the AlAs layers reduces the energy of the  $X_{x,y}$ -states with respect to the  $X_z$ -states [1]. Therefore, the contributions of both the strain and the confinement effect determine the actual configuration of the band gap in these SLs. In particular, Smaoui *et al* have recently shown that a quasi-direct gap and an indirect gap band gap configuration in GaAs/AlAs SLs may be realized for the same well and barrier thicknesses just by varying the layers deformation induced by the lattice-mismatched InGaAs buffer layer [2].

In this paper, we studied deformation of SL layers which arises from the lattice mismatch in short-period GaAs/AlAs SLs with direct energy gap as well as its influence on thermal quenching of photoluminescence (PL) in these structures.

Experiments were carried out on the so-called non-symmetric SLs in which the well thickness is twice the barrier thickness,  $d_w/d_b = 2$ . We have shown previously that under this condition, short-period SLs maintain the direct structure of the band gap even for very small well thicknesses, i.e. non-equilibrium electrons and holes are confined in GaAs layers and recombine through the respective  $\Gamma$ -levels [3]. These structures are, in particular, promising objects for development of light-emitting devices operating in the red region of the visible spectrum [4].

The results of our investigations allowed us to obtain some quantitative information on the structural parameters of SLs (period and deformation of layers) and revealed a correlation between the layer deformation and the activation energy of non-radiative recombination. This correlation is explained in the context of a configuration coordination diagram.

## 2. Experimental details

GaAs/AlAs SLs were grown by molecular beam epitaxy on semi-insulating (100) GaAs substrates. The well width was  $n = 6, 8,$  and  $10$  monolayers (MLs), whereas the barrier width  $m$  was always two times smaller,  $m = n/2$ . Here  $n$  and  $m$  denote, respectively, the well and barrier width expressed in

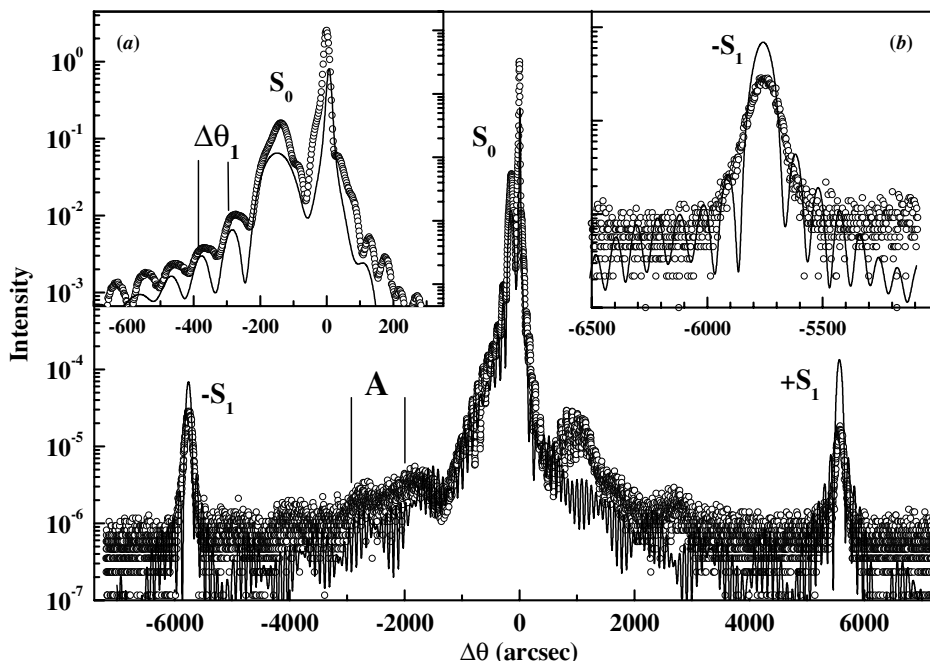


**Figure 1.** Experimental (dots) and simulated (solid lines) x-ray diffraction patterns of the 8/4 SL in the vicinity of the (004) reflection. Insets (a) and (b) show on an enlarged scale fragments of the patterns around the main satellite  $S_0$  and the  $-S_1$  satellite, respectively.

MLs (1 ML = 0.283 nm). We will label the samples as  $n/m$ . The SL periods were 50 for the 10/5 and 8/4 samples and 200 for the 6/3 sample. The SLs were sandwiched between GaAs buffer and cap layers. For the 6/3 SL, a 25 nm  $\text{Ga}_{0.5}\text{Al}_{0.5}\text{As}$  layer was grown on the buffer layer. The growth rate was about  $0.62\text{--}0.7\text{ ML s}^{-1}$ . To improve the interface quality, a growth interruption was applied after each layer deposition.

Structural characterization of the samples was performed by measuring x-ray diffraction patterns for the symmetric (004) and asymmetric (113) reflections using a high-resolution triple-crystal x-ray spectrometer (Philips MRD). A sample was scanned within the angle range of  $\pm 3^\circ$  around the exact Bragg angle position in the so-called  $\omega/2\theta$  scans. The measurements were carried out in a discrete angle regime with a  $2''$  step. The signal-to-noise ratio was about  $10^{-6}$ . To extract sample parameters, the experimental data were fitted using the  $\chi^2$ -method.

The PL experiments were carried out in a cryostat allowing a temperature variation between 4.2 K and room temperature. The samples were excited by an  $\text{Ar}^+$ -ion laser operating in all-lines mode. The PL spectra were recorded using a 0.6 m monochromator, a photomultiplier and a conventional lock-in technique for the PL signal processing.

### 3. Results and discussion

#### 3.1. X-ray diffraction

The experimental and simulated x-ray diffraction patterns of the 8/4 SL recorded for the allowed (004) reflection are shown in figure 1. Since the diffraction patterns for all the samples are similar, we will analyse data on the 8/4 SL, highlighting only differences in the sample characteristics. It is seen from the figure that the main (zeroth-order) peak

dominates the spectrum which is a characteristic feature of a short-period SL [5]. Insets (a) and (b) in figure 1 show on an enlarged scale the x-ray diffraction spectra in the vicinity of the main peak and the  $-S_1$  satellite, respectively. A very good coincidence of experimental and simulated curves is observed. The experimental spectra clearly show the  $\pm S_1$  satellites caused by the SL period as well as other intensity oscillations. The oscillations located near the main SL peak ( $S_0$ ) can be attributed to the so-called fast oscillations. Their appearance evidences a pseudomorphic growth of the SL since the presence of misfit dislocations results in a broadening of the main and higher order satellites [6]. The small full width at half maximum of the  $\pm S_1$  satellites indicates a high structural perfection of the SL [7]. The oscillations labelled A in figure 1 originate from the buffer layer and enable determining its thickness.

The thickness parameters of the GaAs and AlAs layers determined from the distance between the fast oscillations  $\Delta\theta_1$  are summarized in table 1. For all the samples, fluctuations of the SL period and the thickness of individual layers were estimated to be about 0.0003 nm and 0.0001 nm, respectively. For the 10/5 and 8/4 SLs, fitting of the experimental spectra revealed a small deviation of the actual well and barrier thickness from their nominal values. The presence of a 0.003 nm GaAlAs layer was detected in these samples which reflects the interface roughness. A very good agreement between the actual thickness parameters and the nominal ones was obtained for the 6/3 SL. During the fitting of the experimental x-ray diffraction pattern for this sample, there was no necessity to introduce a GaAlAs layer at the GaAs–AlAs interfaces in order to minimize the  $\chi^2$  parameter. This indicates a higher structural quality of the 6/3 SL. Of course, it does not imply that the interfaces are atomically flat because some interface roughness is always present in real samples.

**Table 1.** Experimentally determined parameters of the SL studied: position of the zeroth-satellite  $\Delta\theta_0$ , thickness of layers  $d$  in nm and in monolayers  $n/m$ , average deformation level per SL period ( $\epsilon$ ), deformation level of GaAs ( $\epsilon_w$ ) and AlAs ( $\epsilon_B$ ) layers and activation energy of non-radiative recombination  $E_A$ .

Sample	$\Delta\theta_0$ (degrees)	$d$ (nm)	$n/m$ (MLs)	$\langle\epsilon\rangle$ (%)	$\epsilon_w, \epsilon_B$ (%)	$E_A$ (meV)
10/5	-0.0384	2.863 (GaAs) 0.003 (AlGaAs) 1.414 (AlAs)	10.12/5.0	0.1068	-0.0813 0.178	22
8/4	-0.0397	2.24 (GaAs) 0.003 (AlGaAs) 1.1 (AlAs)	7.92/3.89	0.1038	-0.073 0.175	47
6/3	-0.0344	1.698 (GaAs) 0.849 (AlAs)	6.0/3.0	0.0925	-0.039 0.140	120

The lattice-mismatch induced deformations in the SL layers were analysed using a semi-kinematical approach of the x-ray diffraction theory when the thickness of individual layers is smaller as compared to the extinction length [8]. The inter-plane distance  $\Delta d$  depends on the specific deformation and orientation of the atomic layers  $\Delta d = d_f - d_s$ , where  $d_f$  and  $d_s$  are the film (AlAs) and the substrate (GaAs) thickness, respectively. According to the elasticity theory, the deformations directed parallel ( $\epsilon_{\parallel}$ ) and perpendicular ( $\epsilon_{\perp}$ ) to the crystal surface are determined by a variation of the inter-plane distance in the layer and the substrate:

$$\Delta d/d_s = \epsilon_{\perp} \cos^2 \Psi + \epsilon_{\parallel} \sin^2 \Psi, \quad (1)$$

where  $\Psi$  is the angle between the diffraction plane and the crystal surface.

The angular distance  $\Delta\theta_0$  between the zeroth-order peak of the SL and the main GaAs peak is expressed as follows:

$$-\Delta\theta_0 = k_1 \langle\epsilon_{\perp}\rangle + k_2 \langle\epsilon_{\parallel}\rangle, \quad (2)$$

where

$$\begin{aligned} k_1 &= \cos^2 \Psi \operatorname{tg} \theta_B \pm \sin \Psi \cos \Psi \\ k_2 &= \sin^2 \Psi \operatorname{tg} \theta_B \pm \sin \Psi \cos \Psi, \end{aligned} \quad (3)$$

where  $\theta_B$  is the Bragg angle.

The brackets in equation (2) correspond to the deformation averaged over the SL period. The respective values for the studied samples are given in table 1. The deformation level slightly decreases when going from the 10/5 SL to the 8/4 SL, which differ only by the thickness of well and barrier layers. The deformation decrease is more pronounced for the 6/3 SL. Probably, the smaller deformation value for this sample is observed due to the AlGaAs layer which was deposited on the buffer layer prior to the SL growth. However, additional studies are required to check this assumption.

By measuring the symmetrical (004) and asymmetrical (113) reflections, it is possible to distinguish between  $\epsilon_{\perp}$  and  $\epsilon_{\parallel}$ . Our experiments show that the in-plane deformation of the GaAs layers is smaller than  $\epsilon_{\perp}$  by almost two orders of magnitude which prevents  $\epsilon_{\parallel}$  being estimated accurately. This is in agreement with the results of earlier studies [9]. Therefore, we can conclude that the GaAs and AlAs layers are mainly distorted in the direction, parallel to the SL axis.

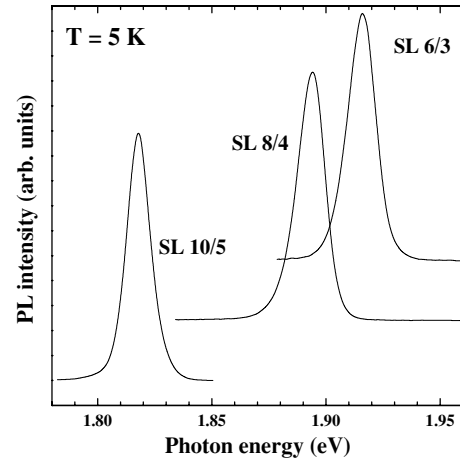


**Figure 2.** PL spectra of the GaAs/AlAs SLs studied taken at 5 K.

### 3.2. Photoluminescence experiments

The PL spectra of the SLs studied taken at 5 K are plotted in figure 2. The spectra are typical for the direct gap GaAs/AlAs SLs: they exhibit one narrow line resulting from annihilation of excitons (electron-heavy hole) confined in the GaAs quantum wells. Increasing temperature leads to both a red shift of the maximum and a spreading of the short-wavelength wing of the PL band towards higher energies. The latter is a characteristic behaviour of the free exciton recombination.

The PL intensity temperature dependence is usually described as

$$I = \frac{I_0}{1 + C \exp(-E_A/k_B T)}, \quad (4)$$

where  $I_0$  is the PL intensity at 0 K,  $E_A$  is the thermal activation energy,  $k_B$  is the Boltzman constant and  $C$  is a constant determined by the radiative to non-radiative lifetime ratio. However, to distinguish between various processes resulting in the PL intensity thermal quenching, it is convenient to rebuild a normal Arrhenius plot  $I = f(1/T)$  in the form  $(I_0/I - 1) = f(1/T)$  [10]. The slopes on this dependence correspond to different activation energies.

For all samples, the temperature increasing up to 35–50 K results in a weak decrease in the PL intensity with an activation energy of 2–3.5 meV (figure 3). This is connected with a progressive thermal release of excitons localized on interface roughness, whereas the free exciton recombination is

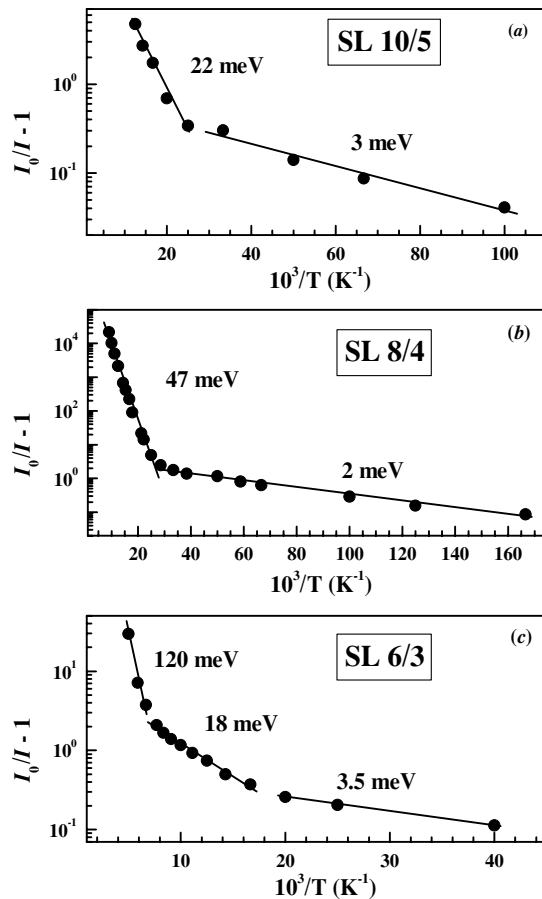


**Figure 3.** PL intensity temperature dependences of the 10/5 (a), 8/4 (b) and 6/3 (c) SLs. Dots are experimental data and solid lines are fits according to equation (4). The corresponding activation energies are indicated at each line.

observed above this temperature. The following luminescence quenching exhibits a quite different behaviour for different samples. In the temperature range of 50–120 K, the PL intensity from the 6/3 SL decreases with an activation energy of about 18 meV which is very close to the calculated exciton binding energy in such samples [11]. A non-radiative recombination process with an activation energy  $E_A \approx 120$  meV governs the PL quenching at  $T > 120$  K. The activation energy significantly decreases on increasing the SL period. For the 8/4 and 10/5 SLs, the non-radiative recombination switches on already at  $T > (35\text{--}40)$  K, and this process competes with the thermal dissociation of excitons making thus impossible a correct estimation of the exciton binding energy from the temperature dependence of the PL intensity. The activation energies obtained are  $E_A \approx 47$  meV and  $E_A \approx 22$  meV for the 8/4 and 10/5 SLs, respectively. These values are much higher than the exciton binding energy.

The observed changes in the activation energy can be related to the SL layer deformation using a configuration coordinate (CC) diagram. The CC diagram is shown in figure 4 for two values of the deformation degree  $\varepsilon_1 < \varepsilon_2$ . Taking into account the change in the deformation for different samples (see table 1), we may suggest that the deformation shifts the excited states curve with respect to the ground state curve. The cross points of the ground and excited states

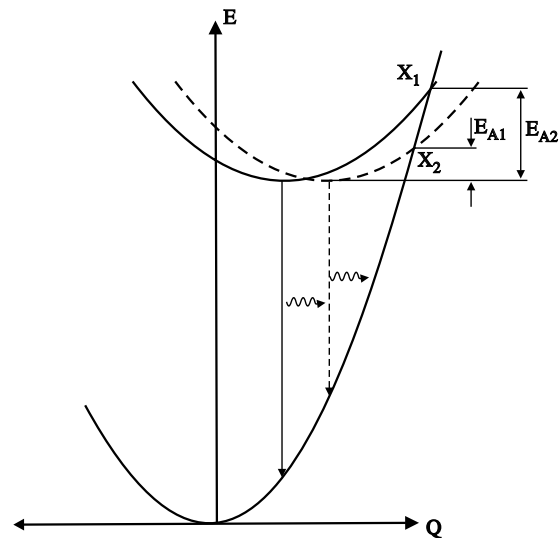


**Figure 4.** A configuration coordinate diagram of the exciton recombination in the GaAs/AlAs SLs. The excited state curves are drawn for deformation degrees  $\varepsilon_1$  (solid line) and  $\varepsilon_2$  (dashed line) ( $\varepsilon_1 < \varepsilon_2$ ).  $E_{A1}$  and  $E_{A2}$  are the activation energies of non-radiative recombination which correspond to the deformation degree  $\varepsilon_1$  and  $\varepsilon_2$ , respectively.

(denoted as  $X_{1,2}$ ) correspond to the height of the energy barriers which a thermally activated exciton should pass through to release its energy via emission of phonons. Therefore, an increasing deformation will lead to a decrease in the thermal activation energy of the non-radiative recombination.

## 4. Conclusions

The structural and optical properties of short-period non-symmetric GaAs/AlAs SLs with a direct energy gap were studied using high-resolution x-ray diffraction and PL techniques. Fitting of the experimental x-ray diffraction patterns in the vicinity of the (004) and (113) reflections allowed us to determine the layer deformation caused by the difference of the lattice constants of GaAs and AlAs and to distinguish between the deformation directed parallel and normal to the SL axis. The deformation was found to decrease with the decreasing SL period. From the temperature dependence of the PL intensity, we found that the activation energy of the non-radiative recombination increases with the decreasing SL period. A correlated behaviour of the activation energy and the deformation degree is discussed within the framework of a configuration coordinate diagram. According to the model proposed, the deformation induces a shift of the excited state curve which corresponds to a decrease of the activation energy.

## Acknowledgments

We would like to thank H T Grahn, R Hey and K Ploog for providing SL samples. This work was supported in part by the Fundamental Research Foundation of the Ministry for Education and Science of Ukraine and the Russian–Ukrainian programme ‘Nanophysics and Nanoelectronics’.

**References**

- [1] Lefebvre P, Gil B, Mathieu H and Planel R 1989 *Phys. Rev. B* **40** 7802
- [2] Smaoui F, Maaref M and Planel R 1999 *Microelectron. J.* **30** 631
- [3] Krylyuk S, Korbutyak D V, Litovchenko V G, Hey R, Grahn H T and Ploog K 1999 *Appl. Phys. Lett.* **74** 2596
- [4] Litovchenko V G, Korbutyak D V, Bercha A I, Kryuchenko Yu V, Krylyuk S G, Grahn H T, Hey R and Ploog K H 2001 *Appl. Phys. Lett.* **78** 4085
- [5] Speriosu V S and Vreelang T 1984 *J. Appl. Phys.* **56** 1591
- [6] Herzog H-J 1993 *Solid State Phenomena* **32-33** 523
- [7] Kyutt R N, Petrashen P V and Sorokin L M 1980 *Phys. Status Solidi a* **60** 381
- [8] Tapfer L and Ploog K 1989 *Phys. Rev. B* **40** 9802
- [9] Cingolani R, Ploog K, Scamarcio G and Tapfer L 1990 *Opt. Quantum Electron.* **22** S201
- [10] Chiari A, Colocci M, Fermi F, Li Yuzhang, Querzoli R, Vinattieri A and Zhuang W 1988 *Phys. Status Solidi b* **147** 421
- [11] Andreani L C and Pasquarello A 1990 *Phys. Rev. B* **42** 8928